Pks5-recombination-mediated surface remodelling in Mycobacterium tuberculosis emergence

Eva C. Boritsch, Wafa Frigui, Alessandro Cascioferro, Wladimir Malaga, Gilles Etienne, Françoise Laval, Alexandre Pawlik, Fabien Le Chevalier, Mickael Orgeur, Laurence Ma, et al.

▶ **To cite this version:**

Eva C. Boritsch, Wafa Frigui, Alessandro Cascioferro, Wladimir Malaga, Gilles Etienne, et al.. Pks5-recombination-mediated surface remodelling in Mycobacterium tuberculosis emergence. Nature Microbiology, 2016, 1 (février 2016), 10.1038/nmicrobiol.2015.19 . pasteur-01265519

HAL Id: pasteur-01265519

https://pasteur.hal.science/pasteur-01265519

Submitted on 1 Feb 2016

HAL is a multi-disciplinary open access archive for the deposit and dissemination of scientific research documents, whether they are published or not. The documents may come from teaching and research institutions in France or abroad, or from public or private research centers.

L'archive ouverte pluridisciplinaire **HAL**, est destinée au dépôt et à la diffusion de documents scientifiques de niveau recherche, publiés ou non, émanant des établissements d'enseignement et de recherche français ou étrangers, des laboratoires publics ou privés.

Distributed under a Creative Commons Attribution - NonCommercial - NoDerivatives 4.0 International License

pks5-recombination-mediated surface remodelling in *Mycobacterium tuberculosis* emergence

Eva C. Boritsch[1], Wafa Frigui[1], Alessandro Cascioferro[1], Wladimir Malaga[2,3], Gilles Etienne[2,3], Françoise Laval[2,3], Alexandre Pawlik[1], Fabien Le Chevalier [1,5], Mickael Orgeur[1], Laurence Ma[4], Christiane Bouchier[4], Timothy P. Stinear[6], Philip Supply[7], Laleh Majlessi[1], Mamadou Daffé[2,3], Christophe Guilhot[2,3,*] and Roland Brosch[1,*].

[1]Institut Pasteur, Unit for Integrated Mycobacterial Pathogenomics, 75015 Paris, France;
[2]CNRS, IPBS (Institut de Pharmacologie et de Biologie Structurale), 31000 Toulouse, France;
[3]Université de Toulouse, UPS, IPBS, 31000 Toulouse, France;
[4]Institut Pasteur, PF1-Plate-Forme Génomique, Paris, France;
[5]University Paris Diderot, Sorbonne Paris Cité, Cellule Pasteur, Paris, France
[6]Department of Microbiology and Immunology, University of Melbourne, Parkville, Victoria, Australia.
[7]Inserm U1019, CNRS UMR8204, Université de Lille, Institut Pasteur de Lille, Center for Infection and Immunity, 59000 Lille, France.

*Corresponding authors: Christophe.Guilhot@ipbs.fr and roland.brosch@pasteur.fr

Mycobacterium tuberculosis is a major, globally spread, aerosol-transmitted human pathogen, thought to have evolved by clonal expansion from a *Mycobacterium canettii*-like progenitor. In contrast, extant *M. canettii* strains are rare, genetically diverse and geographically restricted mycobacteria of only marginal epidemiological importance. Here we show that the contrasting evolutionary success of these two groups is linked to loss of lipooligosaccharide (LOS) biosynthesis and subsequent morphotype changes. Spontaneous smooth-to-rough *M. canettii* variants were found mutated in the polyketide-synthase-encoding *pks5* locus and deficient in LOS synthesis; a phenotype restored by complementation. Importantly, these rough variants showed altered host-pathogen interaction and increased virulence in cellular- and animal-infection models. In one variant, LOS deficiency occurred via homologous recombination between two *pks5* copies and removal of the intervening acyltransferase-encoding gene. The resulting single *pks5* configuration is similar to that fixed in *M. tuberculosis*, known to lack LOS. Our results suggest that *pks5*-recombination-mediated bacterial surface remodelling increased virulence, driving evolution from putative generalist mycobacteria towards professional pathogens of mammalian hosts.

Tuberculosis is a major human infectious disease. Although many aspects of the disease-causing potential of its etiological agent *Mycobacterium tuberculosis* are known[1], our understanding is scant of the molecular events that favoured its evolutionary success as one of the most widely distributed human pathogens. New insights into this question are important for uncovering mechanisms of pathogenesis and new drug targets[2]. Strains of the closely related and phylogenetically early branching *Mycobacterium canettii*, also named smooth tubercle bacilli (STB)[3] are powerful resources to investigate the evolution of *M. tuberculosis* and the *M. tuberculosis* complex (MTBC)[3]. The first strain of *M. canettii* was isolated by Georges Canetti in 1969 and since then less than 100 isolates have been described, most of which have been isolated from tuberculosis patients with a connection to the Horn of Africa[4-7]. Despite their geographic restriction, *M. canettii* strains show much greater genetic variability and are less virulent/persistent than *M. tuberculosis*. Genome comparisons suggest that *M. tuberculosis* evolved by clonal expansion from a pool of *M. canettii*-like tubercle bacilli through the gain of virulence and persistence mechanisms[3,8,9]. While some genomic differences were found to be specific for a single *M. canettii* strain, apparently due to isolated horizontal gene transfer (e.g. the *mce5* operon[3] or the *eptABCD* operon[10], present exclusively in strain STB-J)[3], others are conserved throughout all *M. canettii* strains as a result of phylogenetic ancestry (e.g. *cobF,* present in *M. canettii* and deleted from the MTBC)[3].

Here we investigated phenotypic differences between *M. canettii* and *M. tuberculosis* and focused on the unique, conserved, smooth (S) colony morphotype of *M. canettii*, as opposed to the rough (R) morphotype of MTBC members. Previously, S-morphotypes of non-tuberculous mycobacterial species such as *Mycobacterium avium*[11], *Mycobacterium abscessus*[12], *Mycobacterium kansasii*[13] or *Mycobacterium marinum*[14] have been found to be less virulent than R-morphotypes, raising the question of whether the highly conserved *M. tuberculosis* R-morphotype might have been the result of evolutionary selection, based on host-pathogen interactions favouring a more virulent or persistent phenotype. In other mycobacterial species, S/R variation is often attributed to different kinds of cell surface glycolipids, such as glycopeptidolipids (GPL) for *M. avium*[15] and *M. abscessus*[16,17] or lipooligosaccharides (LOS) for *M. kansasii*[13] and *M. marinum*[14,18,19]. Insights from earlier studies for *M. canettii* have remained abstruse as no specific lipid exclusively present in the S-morphotype has been identified[20], nor has the genetic basis for morphotype variation been determined[4].

Building on recent data from several *M. canettii* genomes[3], here we studied smooth and spontaneously converted R-variants of two different *M. canettii* strains, STB-K (CIPT

140070010) and STB-I (CIPT 140070007)[3], hereafter named $K_{S/R}$ and $I_{S/R}$, respectively. We used whole genome sequencing (WGS) and identified differences in genes of the *pks5* locus, which in *Mycobacterium smegmatis*, *M. marinum* or *M. kansasii* are implicated in LOS biosynthesis[14,21-23]. In this report we uncover the mechanisms underlying the S-to-R morphology change of tubercle bacilli and explore the biological consequences with emphasis on the patho-evolution of *M. tuberculosis.*

RESULTS

Genome comparison of *M. canettii* S- and R-variants

During passaging of different smooth *M. canettii* strains, we observed spontaneous R-morphotype variants for two *M. canettii* strains (I and K). These R-variants were re-passaged three times on solid medium to ensure stable phenotypes and subjected to Illumina-based WGS. The results obtained pointed to morphotype-linked alterations in the *pks5* locus of *M. canettii* S/R variants (Supplementary Tables 1 and 2, Supplementary Note), which was of particular interest given suggested roles for Pks5 polyketide synthases in morphotype changes and LOS production in different mycobacterial species[14,21]. In the LOS-producers *M. marinum*[24] and *M. kansasii*[25], the Pks5-encoding locus harbours two proximal *pks5* homologs separated by one or more interspaced *pks5*-associated gene(s) (Fig. 1A). The genome of *M. canettii* STB-A[3] also shows a twin-*pks5* configuration similar to *M. marinum*. In contrast *M. tuberculosis*, which does not produce LOS only has a single *pks5* and lacks a full-length *pap* ortholog (Fig. 1A).

Recombination of two *pks5* genes in *M. canettii* K_R and *M. tuberculosis*

To characterize the *pks5* locus in strains $I_{S/R,}$ $K_{S/R}$ and *M. tuberculosis* H37Rv we performed long-range PCR using *pks5*-flanking primers, yielding amplicons of ca. 15 kb for both the S- and R-variants of strain I, and 6 kb for *M. tuberculosis* H37Rv, corresponding to the twin- and single-*pks5* configuration, respectively (Fig. 1 A, B). For strain K, however, the prevalent amplicon size of the S-variant was 15 kb, while the size for the R-variant was 6 kb, which was surprising because the previously released STB-K genome sequence assembly[3] indicated only a single *pks5*. The PCR result suggests that the previous WGS-based genome assembly of strain K (NC_019951) contained a misassembly in that region probably due to high sequence identity (> 94 %) between the two *pks5* genes. Similarly, we also confirmed the presence of two *pks5* genes by long-range PCR amplicon-sequencing for *M. canettii* strains D and J, for which previously only one *pks5* was indicated in the released genome sequences NC_019950

and NC_019952, respectively (Supplementary Fig. 1). Hence, the results obtained for S- and R-variants of strain K suggest that K_S contains two *pks5* genes, flanking a gene (*pap*) coding for a putative polyketide-synthase-associated acyltransferase[26], whereas K_R only harbours a single *pks5* and no interspaced *pap* gene.

These findings were supported by results obtained by alignment to the reference sequences of *M. canettii* STB-A and *M. tuberculosis* H37Rv (Supplementary Fig. 2 and Supplementary Note). This analysis suggested that homologous recombination in strain K_R occurred at a site that left intact the typical polyketide-synthase domain structures of Pks5[26,27] (Fig. 1). The observed *pks5* configuration in K_R can thus serve as a model for the situation found in *M. tuberculosis,* where two former *pks5* genes also seem to have coalesced into a single *pks5* gene. In the latter case, the proposed recombination event also left the domain organisation of Pks5 intact, although the site of recombination was apparently different from the site observed for K_R (Fig. 1 and Supplementary Fig. 2B). Further comparisons among different MTBC members[9] showed > 99.93% sequence identity of the single *pks5* gene in these strains, suggesting a unique recombination event in the most recent common ancestor of the MTBC after the separation from an *M. canettii*-like progenitor.

Finally, for strain I, amplicon-sequencing of the *pks5* locus of I_R and I_S confirmed the presence of *pap* and two *pks5* copies in both morphotypes. However, alignment of amplicon-derived sequences indicated the presence of multiple non-synonymous SNPs in both *pks5* genes (6 in *pks5-2* and 3 in *pks5-1*) for the R-variant (Supplementary Fig. 3A), which likely resulted from recombination of the ketosynthase domain regions of the *pks5* copies (Supplementary Fig. 3B). From these data we predicted that these changes likely caused the R-morphotype of I_R.

Pap and Pks5-2 restore the S-morphotype in *M. canettii*

To test if changes in the *pks5* locus were responsible for the S/R variations in *M. canettii*, we transformed strains K_R and I_R, as well as *M. tuberculosis* H37Rv with the integrating cosmid C9, selected from an *M. canettii* STB-A large-fragment genomic library constructed for this purpose in pYUB412. This vector integrates into the *attB* site located in the *glyV*-tRNA of mycobacterial genomes[28]. The 30.5 kb insert of cosmid C9 spans the *pks5* locus of STB-A (Supplementary Fig. 4). Fig. 2 shows that recombinant *M. canettii* strains I_R::C9 and K_R::C9 regained S-morphology that was indistinguishable from their respective S-variants. To refine the region required for S-morphotype restitution, we isolated a second cosmid, named H6 that contains full-length *pap* and *pks5-2* but a 3'-truncated *pks5-1* (Supplementary Fig. 4).

Transformation of I_R and K_R with H6 yielded smooth colonies for both I_R::H6 and K_R::H6 (Supplementary Fig. 5A).

Complementation with a *pks5-2* single gene expression construct restored an S-morphotype for strain I_R::*pks5-2*, but not for K_R::*pks5-2* (Supplementary Figs. 5B and 5C). Moreover, transformation with *pap* was unable to restore smooth colonies in either of the strains despite appropriate protein expression (Supplementary Figs. 5B and 5D). Together, the complementation experiments suggest that *pks5-2* and *pap* are necessary for the S-morphotype in *M. canettii*.

In contrast, R-morphology of *M. tuberculosis* H37Rv remained unchanged upon transformation with cosmid C9 (Fig. 2A) despite correct genomic integration of the cosmid (Fig. 3). Similarly, transformation of other MTBC lineage members with C9 did not yield S-morphotypes (Supplementary Fig. 6). These results suggest that apart from an appropriate *pks5-pap* locus, additional genes intervene in the formation of S-morphotypes in tubercle bacilli.

M. canettii strains synthesize LOS

Analysis of total lipid extracts from a large panel of *M. canettii* strains by thin-layer chromatography (TLC) showed glycoconjugate spots, with TLC mobilities similar to that of LOS from *M. canettii* reference strain CIPT-140010059 (STB-A or *M. canettii* strain A)[29] in all tested strains. Substantial differences in the quantity produced by each strain were observed (Fig. 4A). In contrast, no such glycoconjugates were detected in *M. tuberculosis* H37Rv, consistent with the long-standing knowledge that *M. tuberculosis* does not synthesize LOS (Fig. 4A)[30]. Purification and MALDI-TOF mass spectrometry analysis of LOS from *M. canettii* strains A, K_S and I_S revealed pseudomolecular-ion mass peaks at *m/z* 2530, 2572, and 2614 for LOS from strain K_S (Fig. 4B) and strain A[29], whereas the pattern of strain I_S showed peaks at *m/z* 2516, 2558 and 2600 (Fig. 4B), consistent with the different mobility on TLC (Figs. 4A and 4C). The 14 mass-unit difference indicates strain-specific structural differences, likely due to the absence of one methyl-group from the carbohydrate or the lipid moiety.

The structure of the simplest carbohydrate domain of the *M. canettii* LOS is 2-O-Me-α-L-Fuc*p*(1->3)-β-D-Glc*p*(1->3)-2-O-Me-α-L-Rha*p*(1->3)-2-O-Me-α-L-Rha*p*(1->3)-β-D-Glc*p*(1->3)-4-O-Me-α-L-Rha*p*(1->3)-6-O-Me-α-D-Glc(1<->1)-tri-O-acyl-α-D-Glc (Fig. 4D). This octaglycosyl unit is usually further glycosylated by an incompletely defined *N*-acyl derivative of a 4-amino-4,6-dideoxy-Gal*p* residue to generate a second nonasaccharide-containing glycolipid (LOS 9) (Fig. 4D)[29]. The MALDI-TOF mass spectra of LOS purified

from strains K and A are consistent with the LOS 9 structure. Of note, similar patterns of ion mass peaks were detected in spectra of LOS purified from *M. canettii* strains D, E, F, G, L, and H, while LOS of strain J showed a 14 mass difference, similar to strain I_S (Supplementary Fig. 7).

Rough *M. canettii* variants I and K are deficient in LOS biosynthesis

Having established that all tested *M. canettii* strains synthesized LOS, we next compared the production of these glycoconjugates in the R-variants of I and K. As predicted, I_R was severely impaired in LOS production with only trace amounts detected, and LOS was undetectable in K_R (Fig. 4C and Supplementary Fig. 8). No other differences in polyketide-derived-lipids were observed between the S- and R-variants (Supplementary Fig. 9). Complementation with cosmid C9 restored LOS biosynthesis in recombinant I and K strains (Fig. 4C), whereas recombinant expression of *pks5-2* alone restored the LOS profile in I_R::*pks5-2*, but not in K_R::*pks5-2* (Supplementary Fig. 10A), likely due to the absence of full-length *pap* in K_R::*pks5-2*. Indeed, based on current knowledge on acyl-trehalose biosynthesis in *M. tuberculosis*[31,32], a *pap*-encoded acyltransferase is needed to catalyze the transfer of Pks-produced polymethyl-branched fatty acids onto trehalose.

We also tested LOS production in the MTBC strains complemented with cosmid C9, despite unaffected R-morphotype. LOS was not detected in any of the recombinant *M. tuberculosis* strains (Supplementary Fig. 10B), suggesting that apart from *pks5* recombination and *pap* deletion, in the MTBC additional loss-of-function mutations or insertions/deletions (indels) have occurred in adjacent genes of the LOS-encoding locus that are not covered by cosmid C9 (Supplementary Tables 3 and 4). These results establish that point mutations or recombination/deletion events in the core *pks5-pap* locus of *M. canettii* strains I_R and K_R led to LOS deficiency and R-morphology. The results also explain the R-morphotype of *M. tuberculosis* and open new perspectives for detailed research on the functions of *pks5*-adjacent genes.

Increased fitness and virulence of R-variants in cellular and animal models

Given the identified altered cell surface structure associated with S/R morphology, the question arose whether these changes had an impact on host-pathogen interactions. We thus undertook a series of infection experiments, starting with tests of intracellular replication, a hallmark of mycobacterial virulence. Differentiated human THP-1 macrophages were infected with Sauton-grown *M. canettii* strains K_S, K_R and K_R::C9, as well as K_R::vector-control, up to

five days. While no intracellular growth was observed for K_S and K_R::C9, the R-morphotypes K_R and $K_{R::}$vector-control replicated readily, analogous to *M. tuberculosis* H37Rv (Figs. 5A and 5B). Similar results were obtained when human peripheral blood monocyte-derived macrophages from healthy donors were infected with the different morphotypes (Supplementary Fig. 11A), confirming that the increased fitness advantage of the R-morphotypes was a general phenomenon in human macrophages and not just in THP-1 cells. For murine-derived RAW macrophages a similar trend, but without significant difference was observed (Supplementary Fig. 11B).

To test whether an increased fitness advantage could also be observed *in vivo*, we first infected SCID mice intravenously with 1 x 10^6 CFU of each morphotype. Mice infected with *M. tuberculosis* H37Rv or *M. canettii* K_R had a median survival of 16 and 24 days pi, respectively, while mice infected with strains K_S and K_R::C9 had a longer survival time; on average 31 and 36 days, respectively (Fig. 5C). Higher virulence of R-morphotypes was also observed in the sensitive guinea pig model, using low-dose aerosol infection (Fig. 5D). While in this highly susceptible model, the S-variants of *M. canettii* were already substantially virulent and able to replicate in infected animals, the ratios of the bacterial burden in the lungs at day 42 relative to day 1 were significantly higher for strain K_R than those for the S-morphotypes. Interestingly, for animals infected with K_R::C9 (Fig. 2) we observed more than half of the colonies showing a re-converted R-morphotype, which was never observed in any of our previous *in vitro* experiments, suggesting possible reversion of the usually very stable pYUB412-based integrated genetic complementation[33], due to *in vivo* fitness advantages of R-morphotypes during the long-duration *in vivo* infection assays.

To further investigate the host-pathogen interaction of S- and R-variants, we characterized the inflammatory responses induced in infected phagocytes, as recently performed for S- and R-forms of *M. abscessus*[34,35]. As shown in Figs. 5E and 5F, a potential LOS-dependent anti-inflammatory effect was observed in *M. canettii*-infected bone-marrow derived dendritic cells (BM-DCs) of C57BL/6 mice. Strains K_S and K_R::C9 induced significantly lower secretion of NF-κB-dependent inflammatory cytokines IL-6 and IL-12p40 than K_R. Results with these two cytokines, known to be induced in response to infection with *M. tuberculosis*[36], were also representative for TNF-α and NF-κB-dependent CCL5 and CXCL10 chemokines (Supplementary Fig. 12). In our experimental conditions, most of the responses were dependent on interaction via Toll-like receptor 2 (TLR-2). Smooth variants showed reduced interaction with this crucial innate immune sensor of numerous mycobacterial ligands (Figs. 5 G, 5H and Supplementary Fig. 13). Presence or absence of

LOS thus seems to strongly influence the complex pattern of host-tubercle bacilli interaction, with likely consequences for virulence and pathogenesis.

DISCUSSION

The evolutionary transition for a bacterial population from low-virulence/high genetic diversity towards high-virulence/low genetic diversity is well established for some major human pathogens such as *Yersinia pseudotuberculosis* vs *Yersinia pestis* or *Salmonella enteritidis* vs *Salmonella typhi*[37]. In contrast, the specific genetic changes that led to the emergence of *M. tuberculosis* are less well understood. Here we have exploited the ancestral-state characteristics of *M. canettii* to address this gap in our knowledge[3,6,9]. We show that the transition of *M. tuberculosis* from likely generalist to obligate pathogen was associated with a dramatic change in mycobacterial surface glycolipid composition. The S-to-R morphotype variation we have studied here has been linked with higher virulence in opportunistic pathogenic mycobacteria[11-14] and variation in LOS content has been shown to account for morphology differences in *M. kansasii*[13] or *M. marinum*[14,18,19]. However, earlier studies on *M. canettii* colony morphology have provided inconclusive results. While a study from van Soolingen and coworkers found differences in LOS content between S/R colony variants of an *M. canettii* strain isolated from a 2-year-old Somali child[4], Lemassu and colleagues did not observe a correlation between LOS content and colony morphology in various strains tested[20], likely because the used strains were poor LOS producers with intermediate morphotypes. In this current work we resolve these ambiguities and clearly link LOS biosynthesis with the smooth colony morphotype. We also provide a genetic mechanism for the phenotype that helps explain the evolution of the tubercle bacilli. Our results indicate that recombination of two *pks5* genes associated with deletion of the interspersed *pap* gene evidently was a molecular event that became fixed in the most recent common ancestor of the MTBC after the phylogenetic separation from the *M. canettii* clade (Fig. 6). Indeed, while *M. canettii* strains possess a twin *pks5* and *pap* conformation and synthesize LOS, all members of the classical MTBC contain an abridged *pks5* locus missing a full length *pap* gene and do not produce LOS. Identification of a similar recombination event in a spontaneous R-variant of *M. canettii* K reinforces the likelihood of this evolutionary scenario. Comparable recombination-deletion events also occurred for other genes, e.g. *pknH* (Supplementary Note).

Pks5 is a type-I polyketide synthase and a member of the broader polyketide-synthase family, which in mycobacteria have important functions that range from catalyzing the essential last condensation step of mycolic acid biosynthesis (Pks13)[38] to the synthesis of the

polyketide backbone of phenolic glycolipids (Pks15/1)[39] or the synthesis of mycoketides (Pks12)[40]. In *M. marinum*, the two Pks5 polyketide synthases (Pks5 and Pks5.1) are thought to be involved in the synthesis of polymethyl-branched fatty acids, which are further modified by glycosyltransferases and methyltransferases encoded by genes adjacent to the *pks5* genes[22,23,41] to produce LOS. Indeed, disruption of *pks5* (*MMAR_2340*), analogous to disruptions of the adjacent genes *fadD25* (*MMAR_2341*), *papA4 (MMAR_2343),* and *papA3 (MMAR_2355*) leads to a complete loss of LOS, suggesting that besides the core *pks5-pap* locus, several flanking genes are also involved in the early steps of LOS-biosynthesis[14,18,19,22,23,41,42] (Supplementary Table 3).

Within the group of tubercle bacilli, the overall genetic organization of the orthologous LOS locus is similar between *M. canettii* and the non-functional version in *M. tuberculosis*. However, apart from the recombined *pks5* and the deleted *pap* gene, several flanking genes show SNPs and small indels (Supplementary Table 4), some of which might represent loss-of-function mutations involved in the non-complementation phenotype with cosmid C9 in MTBC members. These findings suggest that after the phylogenetic separation of the MTBC from the *M. canettii*-like progenitor pool, in addition to *pks5* recombination and *pap* deletion, other mutations in genes of the LOS locus accumulated in the MTBC in the absence of selective pressure for sustaining LOS biosynthesis. While LOS production might play an important role in generalist mycobacteria, it appears that its absence might provide a selective advantage for specialized pathogens in the mammalian host.

This conclusion is supported by our different infection experiments, where loss of LOS by *M. canettii* R-variants led to increased virulence in human macrophages and under *in vivo* conditions, particularly for the sensitive guinea pig infection model. These data support a scenario wherein the recombination of *pks5* genes in a common ancestor of the MTBC has contributed to the evolutionary success and host adaptation of the resulting LOS-deprived strains. This finding is in agreement with data for other mycobacterial species, where increased virulence of R-morphotypes relative to S-morphotypes has been reported[11,12,14], although the involved glycolipids are different. In *M. avium,* for example, homologous recombination within the *ser2* gene cluster likely led to phenotype changes linked to loss of GPLs [43]. For *M. abscessus,* a masking effect of GPLs on the outermost layer of the cell wall of the S-morphotype strains has been suggested, which was related to repression of TLR2 responses[34]. Similarly, LOS is located in the outermost layer of the mycobacterial cell envelope[44] and thus might be interacting with other cell wall-associated lipids/glycoconjugates such as phthiocerol dimycocerosates, lipoarabinomannans or the 19-

kD lipoprotein[45], which are important for host-pathogen interaction[46]. At present, it is difficult to speculate by which mechanisms R-variants of tubercle bacilli might have gained a fitness advantage during infection. However, differences we show here in TLR2-mediated inflammatory responses between S- and R-variants of *M. canettii* K suggest that bacterial surface remodelling could well have played an important role in the ancestor of the MTBC during adaptation to mammalian hosts. In this respect, the proposed recombination of *pks5* and deletion of *pap* in a common ancestor of the MTBC adds to previously described differences between *M. canettii* and the MTBC, such as the putative loss of vitamin B12 production due to the *cobF* deletion[3,7,9,47,48], the integration of gene *pe_pgrs33 (rv1818c)*[3], the molecular scars in *pks8/17* and three other gene pairs[3,7,9], or the exchange of the exotoxin-encoding domain in CpnT (Rv3903)[9,49] (Fig. 6). While these reported differences are mainly based on hypotheses formulated during comparative genomics and genome analysis approaches, the virulence differences observed for rough *M. canettii* relative to isogenic LOS-producing smooth *M. canettii* strains now provide first experimental support of our postulated evolutionary model (Fig. 6). Recombination of two ancestral *pks5* genes and consequent remodelling of the bacterial cell surface thus represent key events in the emergence of the professional pandemic pathogen *M. tuberculosis.*

Authors to whom correspondence and requests for materials should be addressed:
Roland Brosch (roland.brosch@pasteur.fr) or Christophe Guilhot
(Christophe.Guilhot@ipbs.fr)

Acknowledgements
We thank Torsten Seemann for initial help with NeighborNet analysis, and Hannes Pouseele for help with mapping and SNP analysis. We are also grateful to Ida Rosenkrands and Giovani Delogu for kindly providing polyclonal anti-SigA antibodies and vector pMV10-25, respectively, and Karim Sébastien for expert assistance in animal care in biosafety-A3 facilities. We acknowledge the support by the European Community's grant 260872, the EU-EFPIA Innovative Medicines Initiative (grant 115337), the Agence National de Recherche (ANR-14-JAMR-001-02) and the Fondation pour la Recherche Médicale FRM (DEQ20090515399 and DEQ20130326471). High-throughput sequencing was performed on the Genomics Platform, member of the "France Génomique" consortium (ANR10-INBS-09-08). R.B. is a member of the LabEx consortium IBEID at the Institut Pasteur. F. L-C was supported by the French Region Ile-de- France (Domaine d'Intérêt Majeur Maladies

Infectieuses et Emergentes) PhD program. E.C.B. was supported by a stipend from the Pasteur–Paris University (PPU) International PhD program and the Institut Carnot Pasteur Maladies Infectieuses.

Author contributions

E.C.B., C.G., L.M. and R.B. designed the study. E.C.B., W.F., F.LC., and A.P. performed mycobacterial phenotypic assays and/or infection experiments. E.C.B., A.C. and R.B. established genetic constructs. W.M., G.E., F.L., M.D. and C. G. generated and/or analysed mycobacterial lipid and lipooligosaccharide profiles. E.C.B., L.Ma, C.B., M.O., T.P.S. and P.S. generated and/or analysed sequence data. E.C.B and L.Majlessi conducted and analysed immune assays. E.C.B., T.P.S., P.S., C.G. and R.B wrote the manuscript, with comments from all authors.

Competing financial interests

P.S. is a consultant for Genoscreen. All other authors declare no competing financial interests.

Accession codes

The WGS-generated reads of the *M. canettii* $I_{S/R}$ and $K_{S/R}$ strains were deposited in the European Nucleotide Archive (ENA) under accession number PRJEB11645 (ERP013045).

Figure legends

Fig. 1. Comparison of *pks5* genomic region of various mycobacterial strains. (A) *pks5* genetic region of *M. kansasii* ATCC 12478, *M. marinum* M, *M. canettii* A and *M. tuberculosis* H37Rv. Percentages on gray lines represent identity values as defined by ClustalW2 between genes of *M. kansasii*, and *M. marinum* or *M. canettii* A and *M. marinum* or *M. tuberculosis* H37Rv. The red arrows indicate location of primers used for long range PCR of *pks5* gene(s) in *M. canettii* strains I and K, as well as in *M. tuberculosis* H37Rv. (B) Results of long range PCR using above-mentioned primers that bind outside the *pks5* genes. *M. tuberculosis* H37Rv (*Mtb*)*; M. canettii* strains: I_S, I_R, K_S and K_R. Note that for strains I_S and I_R unspecific fragments at ~ 12 kb are visible. Data are representative of at least three repetitions. (C) Genetic locus of *pks5* genes in *M. canettii* strains K_S and K_R and potential recombination region in K_R (depicted by black arrows). Percentages on gray lines represent identity values as defined by ClustalW2. (D) Domain organization of the *pks5* genes of *M. canettii* strains K_S

and K_R. Domains were predicted according to the organization *of pks5* of *M. tuberculosis* H37Rv[50] and their respective amino acid positions (AA) are depicted either above or below the particular domains. Sequences of individual domains of *pks5-1* and *pks5-2* were aligned using ClustalW2 and identity values are shown as percentage. Origin of the domains of the recombined *pks5* of *M. canettii* strain K_R is represented in different nuances of gray (light gray originating from *pks5-2* and dark gray from *pks5-1;* medium gray indicates that domains are identical between *pks5-1* and *pks5-2*). Domain abbreviations: ketosynthase (KS), acyltransferase (AT), dehydratase (DH), enoylreductase (ER), ketoreductase (KR) and acyl-carrier protein (ACP).

Figure 2. Complementation of morphology phenotypes of R variants. (A) Colony morphologies of *M. canettii* strains K_S and I_S and their rough mutants K_R and I_R complemented with the whole *pks5* locus (C9) as well as *M. tuberculosis* H37Rv WT and *M. tuberculosis*::C9. Data are representative of at least ten repetitions (plating). Scale bar = 2.5 mm. (B) *M. canettii* strains K_S, K_R and K_R::C9 grown in 7H9 medium supplemented with ADC. Data are representative of at least ten repetitions. Scale bar = 5.0 mm. (C) Ziehl-Neelsen staining of *M. canettii* strains K_S, K_R and K_R::C9. Data are representative of 2 repetitions. Scale bar = 10 μm.

Figure 3. PFGE and Southern hybridization analyses with PCR-derived probes binding either in a conserved domain of *pks5* (middle panel) or within the *pap* gene (right panel). Genomes of strains were digested with *MfeI*, resulting in either a 20 or a 12 kb fragment (black arrows). For all C9-complemented strains, the probe hybridized twice, with fragments of 20 kb and 12 kb confirming the presence of the natural and the vector-integrated *pks5* loci. PFGE gels were run for 16 h with a pulse of 1 s; *M. canettii* A; *M. tuberculosis* H37Rv (*Mtb*); *M. canettii* strains K_S, K_R, K_R::C9; K_R::vector-control; *M. tuberculosis* H37Rv::C9; cosmid C9; M: low-range PFG Marker (NEB). Data are representative of three repetitions.

Figure 4. Deficient LOS production in rough morphotypes. (A) TLC analysis of lipid extracts from various *M. canettii* strains and *M. tuberculosis* H37Rv. Lipid extracts were dissolved in $CHCl_3$ and run in ($CHCl_3$:CH_3OH:H_2O, 60:24:2). Glycolipids were visualized by spraying with anthrone, followed by charring. Insert corresponds to an enhanced contrast picture showing a faint blue spot corresponding to LOS in *M. canettii* A. This experiment was performed at least twice with similar results. (B) MALDI-TOF mass spectra of purified LOS

from *M. canettii* strains I_S and K_S. Note that the mass peak distribution for the LOS component of strain I was 14 mass-units lower than that observed for K and A. Further MS/MS fragmentation analysis showed successive losses of the O-methyl acylated trehalose and oligosaccharides from the 3 major precursor-ions for strain I, and thus suggests that the difference of 14 mass-units resulted from the presence of a rhamnosyl unit in LOS of strain I, instead of a 2-O-Me-rhamnosyl residue linked to the β-glucosyl unit (L-Rha*p*-α1->3-D-Glc*p*-β1->3) present in LOS of strains K. (C) TLC analysis ($CHCl_3$:CH_3OH:H_2O, 60:24:2) of lipid extracts of *M. canettii* strains I_S, I_R, I_R::vector-control, I_R::C9, as well as K_S, K_R, K_R::vector control, K_R::C9 and *M. tuberculosis* H37Rv::C9.. This experiment is representative of two experiments performed independently. LOS = lipooligosaccharide. (D) Structure of lipooligosaccharides (LOS) from *M. canettii.* The acyl substituents, primarily 2L-,4L-dimethylhexadecanoate, 2L-,4L-,6L-,8L-tetramethyloctadecanoate, and 2-methyl-3-hydroxyeicosanoate, are at positions 2,3,6 and 3,4,6 of the terminal glucosyl unit[29].

Figure 5. Survival of morphotypes in different infection models. **(**A-B) Intracellular growth of *M. tuberculosis* H37Rv, *M. canettii* strains K_S, K_R, K_R::C9 and K_R::vector-control in differentiated THP-1 macrophages. THP-1 cells were infected with various strains at an MOI of 0.05 (~ 1 bacterium per 20 cells). CFU of intracellular bacteria were determined 3 h and 3, 4 and 5 days post infection (pi). The figure shows CFU numbers (A) and fold growth rates (B). Data are represented as means and standard deviation of at least four independent experiments. Significance in difference was determined using Two-way *ANOVA* (*$p < 0.05$, **$p < 0.001$, ***$p < 0.0001$). (C) Survival of SCID mice infected with different morphotypes. 1 x 10^6 CFU per mouse of *M. tuberculosis* H37Rv, *M. canettii* strains K_S, K_R or K_R::C9 were IV-injected and survival of mice was monitored. Endpoints were defined as loss of > 20 % of body weight. The initial dose of all strains was comparable with 4.6 x 10^6 CFU/ml for H37Rv, 3.6 x 10^6 CFU/ml for K_S, 4.1 x 10^6 CFU/ml for K_R and 3.3 x 10^6 CFU/ml for K_R::C9. Data represent one experiment with 10 mice per group. (D) Bacterial load of morphotypes in lungs of infected guinea pigs. Guinea pigs were infected via aerosol route with 2.5x10^6 CFU. Lungs of infected animals were homogenized at day 1 and day 42 pi and CFU of different morphotypes were determined. Data represent median with interquartile range of CFU at day 42 divided by CFU at day 1 of two biological replicates with 4 guinea pigs per group (strains K_S and K_R) or 1 experiment with 4 guinea pigs per group (K_R::C9). Significant difference was observed using Kruskal-Wallis test with Dunn's correction (*$p < 0.05$, **$p < 0.01$). (E-F) IL-6 and IL-12p40 production in BM-DCs upon infection with different morphotypes. BM-DCs of

C57BL/6 WT were infected with Sauton-grown *M. tuberculosis* H37Rv, *M. canettii* strains K_S, K_R or K_R::C9 at an MOI of 1. 24 h pi, levels of IL-6 and IL-12p40 in the cell supernatants were determined by ELISA. Note that a dominant inhibitory effect of LOS on the induction of inflammatory responses was excluded since co-infection of BM-DCs with strains K_S and K_R did not result in less cytokine production than infection with *M. canettii* K_R alone. Data are represented as means and standard deviation of three independent experiments. Significance in difference was determined using Mann Whitney test (*$p < 0.05$). (G-H) Differential interaction of S- and R-morphotypes with TLR2. Human TLR2- or TLR4-transfected HEK293 cells were incubated with S- and R-morphotypes at an MOI of 1. At 24 h pi, levels of secreted embryonic alkaline phosphatase reporter gene under the control of NF-κB were measured with a spectrophotometer. PAM3CSK4 (10 µg/ml) and LPS (100 ng/ml) were used as positive controls for TLR2- or TLR4-mediated stimulation, respectively. Data are represented as means and standard deviation of at least three independent experiments. Significance in difference was determined using Mann-Whitney test (***$p < 0.001$). n.s. non-stimulated.

Figure 6. Scheme showing supposed molecular key events in mycobacterial evolution from the recombinogenic *M. canettii* strain pool of putative environmental origin, towards professional pathogens of mammalian hosts evolved by clonal expansion of one emerging sublineage. Network phylogeny inferred among eight *M. canettii* strains used in this study, and 46 MTBC strains by NeighborNet analysis based on genome sequence data. Gene names and arrow shown in grey refer to previously described differences between *M. canettii* strains and MTBC members[9], whereas the *pks5* recombination event is marked by a red arrow. Figure adapted from Bottai et al.[1] and Boritsch et al.[9].

METHODS

Mycobacterial strains and growth conditions

Cloning was performed in LB-grown *Escherichia coli* XL-2 (Stratagene) using hygromycin (200 $\mu g \cdot ml^{-1}$) or kanamycin (50 $\mu g \cdot ml^{-1}$) selection. MTBC and *M. canettii* strains were grown in Middlebrook 7H9 broth (Becton-Dickinson) containing albumin-dextrose-catalase (ADC) or on Middlebrook 7H11 medium (Becton-Dickinson) containing oleic acid-albumin-dextrose-catalase (OADC) or in Sauton medium (when specified) at 37°C. Hygromycin (50 $\mu g \cdot ml^{-1}$) was used for mycobacterial selection.

Genome analysis of S/R morphotype isolates

Mycobacterial DNA was prepared by standard procedures[16,17]. After final ethanol precipitation and washing, DNA was resuspended in TE buffer and used for library preparation and Illumina-based genome sequencing. This approach yielded on average 21 million (I_S and I_R) and 8 million (K_S and K_R) reads per strain, which were then mapped against the corresponding reference sequences of STB-I (ENA WGS project CAOO00000000) and STB-K (NC_019951). Reads were aligned against the reference genomes[3] using SHRiMP[51]. Alignment maps were visualized with Tablet[52] and SNPs were called according to coverage sums and variant frequencies. At least 10 reads had to be matched with a substitution frequency > 0.89 to guarantee the detection of high confidence SNPs. Additional mapping and SNP analysis was performed using BioNumerics v7.6 software (Applied Maths), using parameters pre-calibrated based on re-sequencing data of reference genomes[53].

Network phylogenic analysis of *M. canettii* and MTBC strains

Network phylogeny among *M. canettii* and MTBC strains was inferred by NeighborNet analysis, based on pairwise alignments of whole-genome SNP data. Phylogenetic groupings were identified by split decomposition analysis using the SplitsTree4 software[54].

Long-range PCR and *pks5*-sequencing

pks5 and/or *pap* genes were amplified from chromosomal DNA using Platinum-Taq polymerase (Life Technologies) according to the manufacturer's manual with primers EB-1 TTTATTAATCAGGGAAAGGCGACATCGGA and EB-2 TTTTTATAACCGCCAAGAC AAACTTCATC for annealing at 55°C and elongation at 68°C (10 min). Amplicons were Sanger-sequenced after QIAquick (Quiagen) purification, using primers listed in

supplementary Table **S5**. Amplification of *pks5-1* with the last part of *pap* or amplification of *pks5-2* with the first part of *pap* to verify the presence of both *pks5* genes in the various *M. canettii* strains was performed using Pwo Polymerase (Roche) and the oligos EB-3 GACGAACTACTAGTCGTTGGTAGCG and EB-4 TTTTTATAACCGCCAAGACAAACTTCATC, and EB-5 TTTCAGGGAAAGGCGACATCGGA and EB-6 TTTCGCTACCAACGACTAGTAGTTCGTC, respectively.

Complementation of R-variants

R-variants of *M. canettii* strains K and I, as well as *M. tuberculosis* H37Rv and other MTBC members were transformed with the integrating cosmid C9 and H6 spanning the extended or partial *pks5* locus of *M. canettii* strain A. The C9 and H6 clones were selected from a cosmid library that was constructed in pYUB412[28] by using partially-digested, agarose-embedded genomic DNA[55,56] of *M. canettii* reference strain CIPT 140010059 (STB-A). Clone-inserts were PCR-verified using primers binding in vector- or insert-sequences: (T7-F AGGCATGCAAGCTCAGGATA; T7-R GGATCGGTCCAGTAATCGT and T3-F GCAGAAGCACTAGACGATCC; T3-R GCCGCAATTAACCCTCACTA). Transformed, hygromycin-resistant R-variants that exhibited no S-morphology served as vector-controls. Insert-termini sequencing of these latter clones showed partial insert-loss including the *pks5* region, whereas genes encoding MCAN_15411, MCAN_15421 and part of MCAN 15431 remained present.

For construction of vectors expressing HA-tagged proteins, corresponding genes were amplified with Pwo polymerase (Roche). For the construction of the HA-tagged *pks5-2* expression plasmid, pTTP1b[57] was cut with *Hin*dIII (NEB) to remove the kanamycin resistance cassette and blunt ends were generated using Klenow fragment (NEB). A hygromycin resistance cassette was amplified from pAL70[58] with the oligos AC123 ACAGGCCTGTCGTCGAGGTCCACCAA and AC124 ACAGGCCTGGATGCCAGGGCCTTTCA, cut with *Stu*I and cloned into the digested vector to generate pAL232. The strong mycobacterial promoter of the gene *hsp60* was amplified from chromosomal DNA of *M. tuberculosis* H37Rv with the oligos NheI_HindII_hsp60_F aaaGCTAGCAAGCTTggtgaccacaacgacgcgcccgctttgatc and hsp60_SpeI_EcoRV_XbaI_R aaaTCTAGAgatatcACTAGTtgtcttggccattgcgaagtgattcctcc, the amplified product was cut with *Nhe*I and *Xba*I (NEB) and cloned into *Xba*I-digested pAL232 to generate pEB18. The gene *pks5-2* was amplified from chromosomal DNA of *M. canettii* strain K_S with the oligos

pks5-2_SpeI_F aaaACTAGTGTGGGTAAGGAGAGAACAAAG and pks5-2_HA_PsiI_R aaaTTATAAttaAGCATAATCAGGAACATCATACGGATATGAAGGTGCTGCAATGTC GG. The amplified product was cut with *Spe*I and *Psi*I and cloned into *Spe*I-*Eco*RV digested pEB18. For construction of the HA-tagged *pap* expression system, the plasmid pMV10-25 was first cut with *Nco*I, blunt ended using Klenow fragment (NEB) and subsequently cut with *Nhe*I. The *pap* gene was amplified using the oligos *pap_Spe*I_F aaaACTAGTGTGATCATTGGCGGGGGC and pap_HA_*Psi*I_R aaaTTATAAttaAGCATAATCAGGAACATCATACGGATAGCTAGATACGCGAACTGC TG. The amplified product was digested with *Spe*I and *Psi*I and cloned into the *Nhe*I/ blunt end pMV10-25[59] vector.

Whole cell lysates were generated from cultures grown in Middelbrook 7H9 supplemented with ADC to an OD of 0.6-0.8. Cells were disrupted using a TissueLyser II (Quiagen) and Zirkonia/ Silica beads (BioSpec) and passed through 0.2 µm filter units. Proteins were separated on NuPAGE Novex 10% Bis-Tris gels (Invitrogen) for HA-tagged *pap* and NuPAGE Novex 4-12% Bis-Tris gels (Invitrogen) for HA-tagged *pks5-2*. HA-tagged *pap* was blotted on a nitrocellulose membrane using an iBlot Dry Blotting System (LifeTechnologies), while *pks5-2* was blotted on nitrocellulose membranes using a wet transfer system for 2 h at 100 V at 4°C. Membranes were blocked in 5% milk powder in TBS and subsequently incubated with either mouse anti-HA (anti-HA.11; Covance) or rabbit anti-SigA (Statens Serum Institute, Copenhagen, Denmark) primary antibody. Bound antibodies were detected using a horseradish peroxidase-conjugated sheep anti-mouse or donkey anti-rabbit (Amersham ECL) antibody and the chemiluminescent signal was developed with a SuperSignal West Femto Maximum Sensitivity Substrate (Thermo Scientific). Image acquisition was performed with an Azure c300 (Azure Biosystems).

Ziehl-Neelsen staining

Mycobacteria were grown to an OD of 0.4, smeared on glass slides and killed at 95°C (1 h). After heat-fixation with 90% ethanol, mycobacteria were stained with carbol-fuchsin and heated (10 min). After washing, glass slides were incubated with sulphuric acid (25%) (2 min), washed and incubated with 90% ethanol (5 min), washed and counter-stained with methylene blue (2 min).

PFGE and Southern Blot hybridization

Genomic DNA in agarose-plugs, prepared as described[55], was *Mfe*I-digested, separated by pulsed-field gel electrophoresis (Biorad CHEF II, pulse 1 s for 16 h at 6 $V \cdot cm^{-1}$) and transferred onto Hybond-C-Extra nitrocellulose (GE), as described[55]. Hybridization was performed with [α-^{32}P]dCTP-labeled PCR-probes at 68°C in 6xSSC/ 0,5% SDS/ 0.01 M EDTA/ 5xDenhardt's solution/ 100 $mg \cdot ml^{-1}$salmon-sperm DNA. After washing, membranes were exposed to phosphorimager screens, which were scanned in a STORM phosphorimager. Probes were amplified from *M. tuberculosis* DNA using *pks5* primers (pks5-F GTTGTGGGAGGCGTTGCT; pks5-R GAAACGTCGAACGCATGAC) or from *M. canettii* K_S using *pap* primers (pap-F CTCGATTATTCACGGCTGGT; pap-R CGTATAGCCCGGTGATCAAC).

Extraction and analysis of lipooligosaccharides

Mycobacterial cells obtained from 7H9-grown cultures were exposed to $CHCl_3/CH_3OH$ (1:2, v/v) for 48h to kill bacteria. Lipids were extracted following previously described protocols[14,21] and separated by TLC. Finally, glycolipids were visualized by spraying the plates with a 0.2% anthrone solution (w/v) in concentrated H_2SO_4, followed by heating. The previously described LOS of *M. canettii* strain CIPT 140010059 was used as standard[29]. Crude lipid extracts were subjected to chromatography on a Sep-Pak Florisil cartridge and eluted at various concentrations of CH_3OH (0, 5, 10, 15, 20, 30%) in $CHCl_3$. Each fraction was analyzed by TLC on Silica Gel G60 using $CHCl_3/CH_3OH/H_2O$ (30:12:1, v/v/v) as solvent and glycolipids were visualized as described above.

MALDI-TOF/TOF-MS and MS/MS analyses were conducted in the positive ionization and reflectron mode by accumulating 10 spectra of 250 laser shots, using the 5800 MALDI TOF/TOF Analyser (Applied Biosystems/Absciex) equipped with a Nd:Yag laser (349nm). For MS and MS/MS data acquisitions, uniform, continuous, and random stage motion was selected at a fixed laser intensity of 4000 (instrument-specific units) and 400 Hz pulse rate and 6000 (instrument-specific units) and 1000Hz, respectively. For MS/MS data acquisition, the fragmentation of selected precursor-ions was performed at collision energy of 1 kV. Lipid samples were dissolved in chloroform and spotted onto the target plate as 0.5 µl droplets, followed by the addition of 0.5 µl matrix solution (10 mg of 2,5-dihydroxybenzoic acid [Sigma-Aldrich]/ml in $CHCl_3/CH_3OH$, 1/1 [vol/vol]. Samples were allowed to crystallize at room temperature. Spectra were externally calibrated using lipid standards.

Alkaline hydrolysis of purified LOS and total extractable lipids from the various strains was performed with 1M sodium methanolate for 1h at 37°C. After neutralization with

glacial acetic acid, the mixture was dried under stream of nitrogen and lipids were extracted with diethyl ether and washed twice with water. The resulting fatty acid methyl esters were converted to trimethylsilyl (TMS) derivatives, using a mixture of pyridine/hexamethyldisilazane/trimethylchlorosilane (6:4:2, v/v/v).

GC-MS analyses were performed using a Thermo TraceGCultra chromatograph coupled with an ISQ mass spectrometer. Chromatographic separations of the TMS derivatives of the fatty acid methyl esters were obtained using an Inferno ZB5HT column of 15m. Helium was the carrier gas at constant flow rate of 1.2mL min^{-1}. The oven temperature program was started at 120°C, ramped to 380°C at 10°C/min (with final isothermal step of 5min at 380°C). The temperature of the injector was 220°C and injection of 1µl of samples in petroleum ether was performed in a split mode (ratio of 20:1). EI mass spectra were recorded using electron energy of 70eV from 60 to 600 with a transfer line maintained at 275°C.

To visualize various polyketide-derive lipids, including acyl-trehaloses such diacyltrehaloses (DAT), polyacyltrehaloses (PAT), sulfolipids (SL), phenolic glycolipids (PGL) or lipooligosaccharides (LOS) from different *M. canettii* strains metabolic labelling with ^{14}C propionate was used. For this TLC analysis, *M. canettii* strains were grown to the exponential phase in 10 mL 7H9 liquid medium supplemented with ADC and 0.05% Tween 80 and labelled by incubation with 0.4 µCi.ml^{-1} [1-^{14}C] propionate for 24 h. The TLC plates were run in $CHCl_3/CH_3OH/H_2O$ (60/16/2) for DAT and SL and $CHCl_3/CH_3OH$ (99/1) for PAT. Labelled lipids were visualized with a Typhoon PhosphorImager (Amersham Biosciences).

Macrophage infections

THP-1 (TIB-202D) human monocyte-like cells were purchased from ATCC, directly amplified and stocked in liquid nitrogen. Only low passage cells (passage number <11) were used in the experiments. The purchased THP-1 cell line has been authenticated and tested for microbial contaminants, including mycoplasma, by ATCC. For the experiments, THP-1 were cultivated in RPMI 1640, GlutaMAX (Life Technologies) containing 10 % heat-inactivated fetal bovine serum (Life Technologies), seeded at a density of $7.5x10^4$ cells per well in 96 well plates and differentiated into macrophages through incubation with 50 mM PMA for 3 days. For infection, bacteria grown in Sauton medium without shaking were sonicated, added to the macrophages at an MOI of 0.05, (~ 1 bacterium per 20 THP-1 cells) and incubated for 2 h. Sauton medium was used, as it allows the production of more complex polar lipids[18]. After phagocytosis, 0.1 mg·ml^{-1} amikacin was added for 1 h to remove extracellular bacteria and

cells were incubated for up to 6 days at 37˚C and 5% CO_2. At various time points macrophages were lysed with 0.1% Triton-X100 in PBS and lysates plated in serial dilutions on 7H11+OADC plates to determine intracellular survival of bacteria in CFU. Experiments were performed as at least four biological replicates, each done in triplicate (technical replicates).

Additional infection experiments were conducted using Raw murine macrophages as well as Human monocyte-derived macrophages (hMDMs). Raw cells were cultivated in RPMI 1640 Medium, GlutaMAX (Gibco, Life Technologies) supplemented with 5 % heat-inactivated fetal bovine serum (Gibco, Life Technologies) and seeded one day before infection. In parallel, hMDMs were obtained from buffy coats by centrifugation of blood from healthy human donors in lymphocyte separation medium (Eurobio) and further isolation of $CD14^+$ monocytes from the mononuclear cell fraction using CD14 microbeads (Miltenyi Biotec). Monocytes were differentiated into macrophages in the presence of rhM-CSF (50 ng/ml; R&D Systems). At the day of infection mycobacterial strains grown in Sauton medium without shaking were sonicated, added to the macrophages at a MOI of 1:20, and incubated for 2 hrs at 37˚C and 5% CO_2. After phagocytosis, infected macrophages were incubated with 0.1 $mg \cdot ml^{-1}$ amikacin for 1 h to remove extracellular bacteria and finally incubated for 6 days in new RPMI supplemented with 10 % FBS for hMDMs and 1% for Raw cells at 37˚C and 5 % CO_2. At selected time points macrophages were lysed with 0.1 % Triton-X100 in PBS and bacteria were plated in serial dilutions on 7H11 plates supplemented with OADC to determine CFU counts. Buffy coats were obtained from healthy donors after informed consent (Etablissement Français du Sang). Three biological replicates were performed, each done in triplicate (technical replicates).

Animal infection studies

Six-week-old female SCID mice (Charles River) were infected intravenously with 200 µl of $5x10^6$ bacteria/mouse and survival of mice was monitored. Humane endpoints were defined as loss of > 20 % of body-weight. The experiment was performed once, using 10 mice per strain (technical replicates). In a second well-established mycobacterial infection model, five to six week-old female guinea pigs (Hartley; Charles River) were aerosol-infected using 5 ml of a suspension containing $5x10^5$ $bacteria \cdot ml^{-1}$. Six weeks post-infection, animals were killed and organs homogenized using a gentleMACS Dissociator (Miltenyi Biotec) and gentleMACS M tubes. Bacterial loads in organs were determined by plating serial dilutions of organ homogenates on solid medium. The number of animals included in the experiments

(sample size choice) was determined by taking into account the rule of 3Rs (replacement, reduction, refinement) and statistical requirements. As regards randomization and blinding, CFU counts were recorded in parallel by different investigators.

Cytokine and chemokine assays and HEK-Blue cell reporter assay

ELISA and ProcartaPlex Luminex immunoassay from culture supernatants of infected BM-DCs was performed as previously described[60], and/or according to the manufacturer's instructions (ProcartaPlex Luminex Immunoassay). mAbs specific to IL-12p40 and IL-6 were from BD Biosciences. Reagents for quantitative ProcartaPlex Luminex immunoassay were from affymetrix eBioscience. ELISA experiments were performed as three biological replicates, while Luminex analyses were performed as two independent biological replicates, each done in duplicate. Signal acquisition was performed on pooled duplicates.

HEK-TLR2 and HEK-TLR4 cells (InvivoGen) were grown in DMEM medium (Gibco Life Technologies) supplemented with 10% FBS, 100 $\mu g \cdot ml^{-1}$ Normocin and 1X HEK-Blue Selection. TLR stimulation assay was performed according to the manufacturer's protocol. 10 $\mu g \cdot ml^{-1}$ PAM3CSK4 served as positive control for HEK-TLR2 and 100 $ng \cdot ml^{-1}$ LPS as positive control for HEK-TLR4. Experiments were performed as at least three biological replicates.

Compliance with regulations on animal welfare and ethics

Animal studies were performed in agreement with European and French guidelines (Directive 86/609/CEE and Decree 87–848 of 19 October 1987) after approval by the Institut Pasteur Safety Committee (Protocol 11.245) and local ethical committees (CNREEA 2012-0061; CETEA 2013-0036).

References:

1 Bottai, D., Stinear, T. P., Supply, P. & Brosch, R. Mycobacterial Pathogenomics and Evolution *Microbiology Spectrum* **2**, MGM2-0025-2013 (2014).

2 Le Chevalier, F., Cascioferro, A., Majlessi, L., Herrmann, J. L. & Brosch, R. *Mycobacterium tuberculosis* evolutionary pathogenesis and its putative impact on drug development. *Future Microbiol.* **9:969-85.**, (2014).

3 Supply, P. *et al.* Genomic analysis of smooth tubercle bacilli provides insights into ancestry and pathoadaptation of *Mycobacterium tuberculosis*. *Nat Genet* **45**, 172-179 (2013).

4 van Soolingen, D. *et al.* A novel pathogenic taxon of the *Mycobacterium tuberculosis* complex, Canetti: characterization of an exceptional isolate from Africa. *Int J Syst Bacteriol* **47**, 1236-1245. (1997).

5 Gutierrez, M. C. *et al.* Ancient origin and gene mosaicism of the progenitor of Mycobacterium tuberculosis. *PLoS Pathog.* **1**, e5.

6 Koeck, J. L. *et al.* Clinical characteristics of the smooth tubercle bacilli 'Mycobacterium canettii' infection suggest the existence of an environmental reservoir. *Clin Microbiol Infect* **17**, 1013-1019 (2011).

7 Blouin, Y. *et al.* Progenitor "*Mycobacterium canettii"* Clone Responsible for Lymph Node Tuberculosis Epidemic, Djibouti. *Emerg Infect Dis* **20**, 21-28, (2014).

8 Dormans, J. *et al.* Correlation of virulence, lung pathology, bacterial load and delayed type hypersensitivity responses after infection with different *Mycobacterium tuberculosis* genotypes in a BALB/c mouse model. *Clin Exp Immunol.* **137**, 460-468. (2004).

9 Boritsch, E. C. *et al.* A glimpse into the past and predictions for the future: the molecular evolution of the tuberculosis agent. *Mol Microbiol.* **93**, 835-852. (2014).

10 Panas, M. W. *et al.* Noncanonical SMC protein in Mycobacterium smegmatis restricts maintenance of *Mycobacterium fortuitum* plasmids. *Proc Natl Acad Sci U S A.* **111**, 13264-13271. (2014).

11 Kansal, R. G., Gomez-Flores, R. & Mehta, R. T. Change in colony morphology influences the virulence as well as the biochemical properties of the *Mycobacterium avium* complex. *Microb Pathog* **25**, 203-214, (1998).

12 Catherinot, E. *et al.* Hypervirulence of a rough variant of the *Mycobacterium abscessus* type strain. *Infect Immun* **75**, 1055-1058, (2007).

13 Belisle, J. T. & Brennan, P. J. Chemical basis of rough and smooth variation in mycobacteria. *J Bacteriol.* **171**, 3465-3470. (1989).

14 van der Woude, A. D. *et al.* Unexpected link between lipooligosaccharide biosynthesis and surface protein release in *Mycobacterium marinum*. *J Biol Chem* **287**, 20417-20429, (2012).

15 Barrow, W. W. & Brennan, P. J. Isolation in high frequency of rough variants of Mycobacterium intracellulare lacking C-mycoside glycopeptidolipid antigens. *J Bacteriol.* **150**, 381-384. (1982).

16 Howard, S. T. *et al.* Spontaneous reversion of *Mycobacterium abscessus* from a smooth to a rough morphotype is associated with reduced expression of glycopeptidolipid and reacquisition of an invasive phenotype. *Microbiology* **152**, 1581-1590, (2006).

17 Pawlik, A. *et al.* Identification and characterization of the genetic changes responsible for the characteristic smooth-to-rough morphotype alterations of clinically persistent *Mycobacterium abscessus*. *Mol.Microbiol.***90**, 612-629. (2013).

18 Burguiere, A. *et al.* LosA, a key glycosyltransferase involved in the biosynthesis of a novel family of glycosylated acyltrehalose lipooligosaccharides from *Mycobacterium marinum*. *J Biol Chem.* **280**, 42124-42133. (2005).

19 Ren, H. *et al.* Identification of the lipooligosaccharide biosynthetic gene cluster from *Mycobacterium marinum*. *Mol Microbiol* **63**, 1345-1359 (2007).

20 Lemassu, A., Levy-Frebault, V. V., Laneelle, M. A. & Daffe, M. Lack of correlation between colony morphology and lipooligosaccharide content in the *Mycobacterium tuberculosis* complex. *J Gen Microbiol.* **138**, 1535-1541. (1992).

21 Etienne, G. *et al.* Identification of the polyketide synthase involved in the biosynthesis of the surface-exposed lipooligosaccharides in mycobacteria. *J Bacteriol* **191**, 2613-2621 (2009).

22 Nataraj, V. *et al.* MKAN27435 is required for the biosynthesis of higher subclasses of lipooligosaccharides in *Mycobacterium kansasii*. *PLoS One.* **10**, e0122804. (2015).

23 Minnikin, D. E. *et al.* in *Tuberculosis - Expanding Knowledge* (ed W. Ribon) Ch. 7, (InTech, 2015).

24 Stinear, T. P. *et al.* Insights from the complete genome sequence of *Mycobacterium marinum* on the evolution of *Mycobacterium tuberculosis*. *Genome Res* **18**, 729-741. (2008).

25 Wang, J. *et al.* Insights on the Emergence of *Mycobacterium tuberculosis* from the Analysis of *Mycobacterium kansasii*. *Genome Biol Evol.* **7**, 856-870. doi: 810.1093/gbe/evv1035. (2015).

26 Quadri, L. E. Biosynthesis of mycobacterial lipids by polyketide synthases and beyond. *Crit Rev Biochem Mol Biol.* **49**, 179-211. (2014).

27 Rousseau, C. *et al.* Virulence attenuation of two Mas-like polyketide synthase mutants of *Mycobacterium tuberculosis*. *Microbiology.* **149**, 1837-1847. (2003).

28 Bange, F. C., Collins, F. M. & Jacobs, W. R., Jr. Survival of mice infected with *Mycobacterium smegmatis* containing large DNA fragments from *Mycobacterium tuberculosis*. *Tuber Lung Dis* **79**, 171-180. (1999).

29 Daffe, M., McNeil, M. & Brennan, P. J. Novel type-specific lipooligosaccharides from *Mycobacterium tuberculosis*. *Biochemistry.* **30**, 378-388. (1991).

30 Angala, S. K., Belardinelli, J. M., Huc-Claustre, E., Wheat, W. H. & Jackson, M. The cell envelope glycoconjugates of *Mycobacterium tuberculosis*. *Crit Rev Biochem Mol Biol.* **49**, 361-399. (2014).

31 Onwueme, K. C., Ferreras, J. A., Buglino, J., Lima, C. D. & Quadri, L. E. Mycobacterial polyketide-associated proteins are acyltransferases: proof of principle with *Mycobacterium tuberculosis* PapA5. *Proc Natl Acad Sci U S A.* **101**, 4608-4613. (2004).

32 Bhatt, K., Gurcha, S. S., Bhatt, A., Besra, G. S. & Jacobs, W. R., Jr. Two polyketide-synthase-associated acyltransferases are required for sulfolipid biosynthesis in *Mycobacterium tuberculosis*. *Microbiology.* **153**, 513-520. (2007).

33 Bottai, D. *et al.* Increased protective efficacy of recombinant BCG strains expressing virulence-neutral proteins of the ESX-1 secretion system. *Vaccine.* **33**, 2710-2718. (2015).

34 Rhoades, E. R. *et al. Mycobacterium abscessus* Glycopeptidolipids mask underlying cell wall phosphatidyl-myo-inositol mannosides blocking induction of human macrophage TNF-alpha by preventing interaction with TLR2. *J Immunol* **183**, 1997-2007, (2009).

35 Roux, A. L. *et al.* Overexpression of proinflammatory TLR-2-signalling lipoproteins in hypervirulent mycobacterial variants. *Cell Microbiol* **13**, 692-704, (2011).

36 Robinson, R. T., Orme, I. M. & Cooper, A. M. The onset of adaptive immunity in the mouse model of tuberculosis and the factors that compromise its expression. *Immunol Rev.* **264**, 46-59. (2015).

37 Achtman, M. Insights from genomic comparisons of genetically monomorphic bacterial pathogens. *Philos Trans R Soc Lond B Biol Sci* **367**, 860-867 (2012).

38 Portevin, D. *et al.* A polyketide synthase catalyzes the last condensation step of mycolic acid biosynthesis in mycobacteria and related organisms. *Proc Natl Acad Sci U S A* **101**, 314-319. (2004).

39 Constant, P. *et al.* Role of the *pks15/1* gene in the biosynthesis of phenolglycolipids in the *Mycobacterium tuberculosis* complex. Evidence that all strains synthesize glycosylated *p*-hydroxybenzoic methyl esters and that strains devoid of phenolglycolipids harbor a frameshift mutation in the *pks15/1* gene. *J Biol Chem* **277**, 38148-38158, (2002).

40 Matsunaga, I. *et al. Mycobacterium tuberculosis pks12* produces a novel polyketide presented by CD1c to T cells. *J Exp Med.* **200**, 1559-1569. (2004).
41 Rombouts, Y. *et al.* Fatty acyl chains of *Mycobacterium marinum* lipooligosaccharides: structure, localization and acylation by PapA4 (MMAR_2343) protein. *J Biol Chem.* **286**, 33678-33688. (2011).
42 Alibaud, L. *et al.* Increased phagocytosis of *Mycobacterium marinum* mutants defective in lipooligosaccharide production: a structure-activity relationship study. *J Biol Chem.* **289**, 215-228. (2014).
43 Eckstein, T. M., Inamine, J. M., Lambert, M. L. & Belisle, J. T. A genetic mechanism for deletion of the *ser2* gene cluster and formation of rough morphological variants of *Mycobacterium avium*. *J Bacteriol* **182**, 6177-6182 (2000).
44 Ortalo-Magne, A. *et al.* Identification of the surface-exposed lipids on the cell envelopes of *Mycobacterium tuberculosis* and other mycobacterial species. *J Bacteriol* **178**, 456-461 (1996).
45 Mortaz, E. *et al.* Interaction of Pattern Recognition Receptors with *Mycobacterium tuberculosis*. *J Clin Immunol* **14**, 14 (2014).
46 Cambier, C. J. *et al.* Mycobacteria manipulate macrophage recruitment through coordinated use of membrane lipids. *Nature.* **505**, 218-222. (2014).
47 Gopinath, K., Moosa, A., Mizrahi, V. & Warner, D. F. Vitamin B(12) metabolism in *Mycobacterium tuberculosis*. *Future Microbiol* **8**, 1405-1418 (2013).
48 Young, D. B., Comas, I. & de Carvalho, L. P. Phylogenetic analysis of vitamin B12-related metabolism in Mycobacterium tuberculosis. *Front Mol Biosci.* **2**, 6. (2015)
49 Danilchanka, O. *et al.* An outer membrane channel protein of *Mycobacterium tuberculosis* with exotoxin activity. *Proc Natl Acad Sci U S A.* **111**, 6750-6755. (2014).
50 Delahay *et al.* The coiled-coil domain of EspA is essential for the assembly of the type III secretion translocon on the surface of enteropathogenic *Escherichia coli*. *J Biol Chem.* **274**, 35969-35974.

References Methods

51 David, M., Dzamba, M., Lister, D., Ilie, L. & Brudno, M. SHRiMP2: sensitive yet practical SHort Read Mapping. *Bioinformatics.* **27**, 1011-1012. (2011).
52 Milne, I. *et al.* Using Tablet for visual exploration of second-generation sequencing data. *Brief Bioinform.* **14**, 193-202. (2013).
53 Pouseele, H. & Supply, P. Accurate whole-genome sequencing-based epidemiological surveillance of mycobacterium tuberculosis. *Methods in Microbiology*. doi:10.1016/bs.mim.2015.04.001 (2015).
54 Huson, D. H. & Bryant, D. Application of phylogenetic networks in evolutionary studies. *Mol Biol Evol* **23**, 254-267 (2006).
55 Brosch, R. *et al.* Comparative genomics uncovers large tandem chromosomal duplications in Mycobacterium bovis BCG Pasteur. *Yeast* **17**, 111-123. (2000).
56 Brosch, R. *et al.* Use of a Mycobacterium tuberculosis H37Rv bacterial artificial chromosome library for genome mapping, sequencing, and comparative genomics. *Infect Immun* **66**, 2221-2229 (1998).
57 Pham, T. T., Jacobs-Sera, D., Pedulla, M. L., Hendrix, R. W. & Hatfull, G. F. Comparative genomic analysis of mycobacteriophage Tweety: evolutionary insights and construction of compatible site-specific integration vectors for mycobacteria. *Microbiology.* **153**, 2711-2723 (2007).

58 Cascioferro, A. *et al.* Xer site-specific recombination, an efficient tool to introduce unmarked deletions into mycobacteria. *Appl Environ Microbiol* **76**, 5312-5316 (2010).
59 Delogu, G. *et al.* Rv1818c-encoded PE_PGRS protein of Mycobacterium tuberculosis is surface exposed and influences bacterial cell structure. *Mol Microbiol* **52**, 725-733 (2004).
60 Majlessi, L. *et al.* Influence of ESAT-6 Secretion System 1 (RD1) of *Mycobacterium tuberculosis* on the Interaction between Mycobacteria and the Host Immune System. *J Immunol* **174**, 3570-3579 (2005).

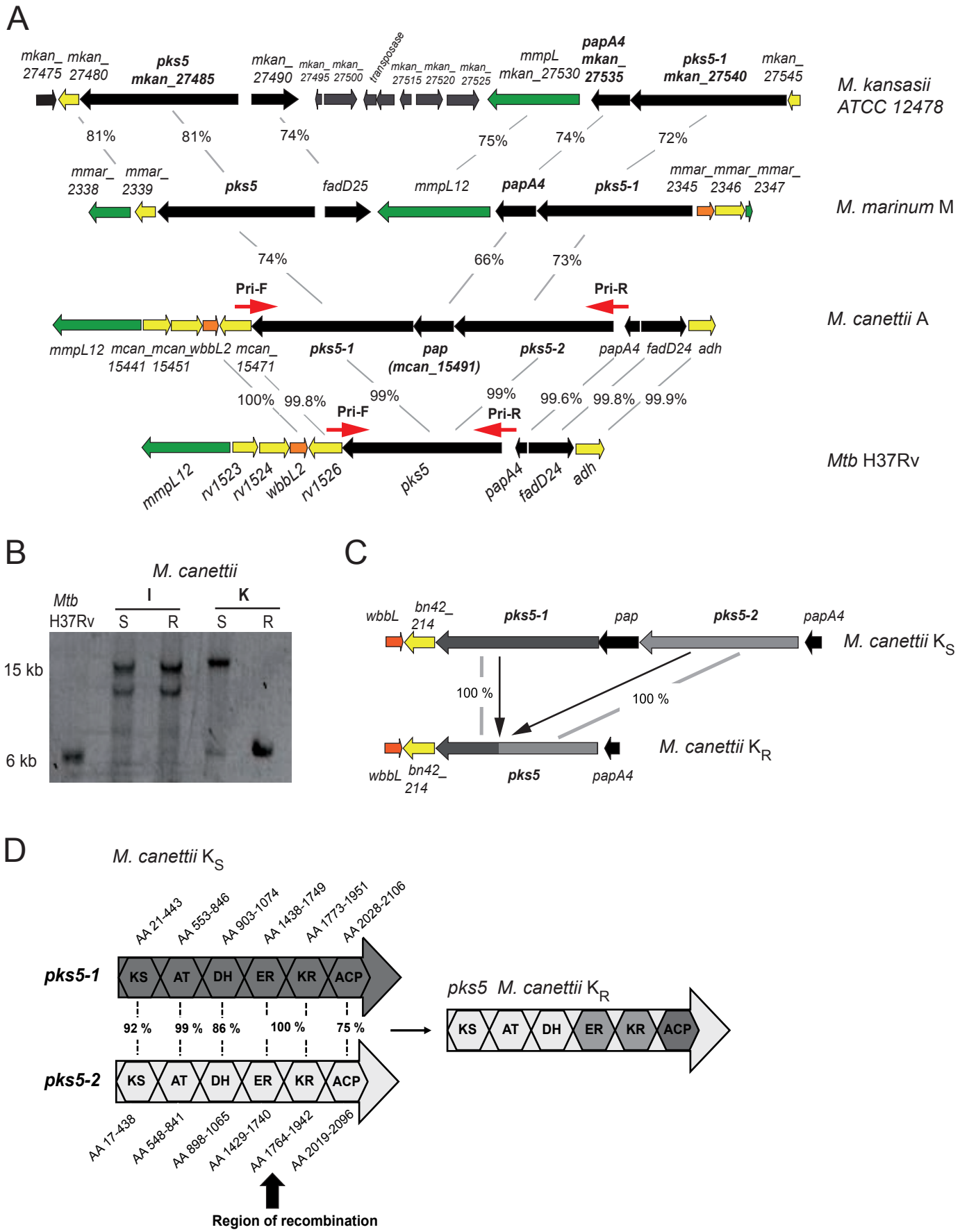
A
mkan_ 27475
mkan_ 27480
pks5 mkan_27485
mkan_ 27490
mkan_ 27495
mkan_ 27500
transposase
mkan_ 27515
mkan_ 27520
mkan_ 27525
mmpL mkan_27530
papA4 mkan_ 27535
pks5-1 mkan_27540
mkan_ 27545
M. kansasii ATCC 12478
81%
81%
74%
75%
74%
72%
mmar_ 2338
mmar_ 2339
pks5
fadD25
mmpL12
papA4
pks5-1
mmar_ 2345
mmar_ 2346
mmar_ 2347
M. marinum M
74%
66%
73%
Pri-F
Pri-R
mmpL12
mcan_ 15441
mcan_ 15451
wbbL2
mcan_ 15471
pks5-1
pap (mcan_15491)
pks5-2
papA4
fadD24
adh
M. canettii A
100%
99.8%
99%
99%
99.6%
99.8%
99.9%
Pri-F
Pri-R
mmpL12
rv1523
rv1524
wbbL2
rv1526
pks5
papA4
fadD24
adh
Mtb H37Rv
B
M. canettii
Mtb H37Rv
I
K
S
R
S
R
15 kb
6 kb
C
wbbL
bn42_ 214
pks5-1
pap
pks5-2
papA4
M. canettii K_S
100 %
100 %
M. canettii K_R
wbbL
bn42_ 214
pks5
papA4
D
M. canettii K_S
AA 21-443
AA 553-846
AA 903-1074
AA 1438-1749
AA 1773-1951
AA 2028-2106
pks5-1
KS
AT
DH
ER
KR
ACP
92 %
99 %
86 %
100 %
75 %
pks5-2
KS
AT
DH
ER
KR
ACP
AA 17-438
AA 548-841
AA 898-1065
AA 1429-1740
AA 1764-1942
AA 2019-2096
pks5 M. canettii K_R
KS
AT
DH
ER
KR
ACP
Region of recombination

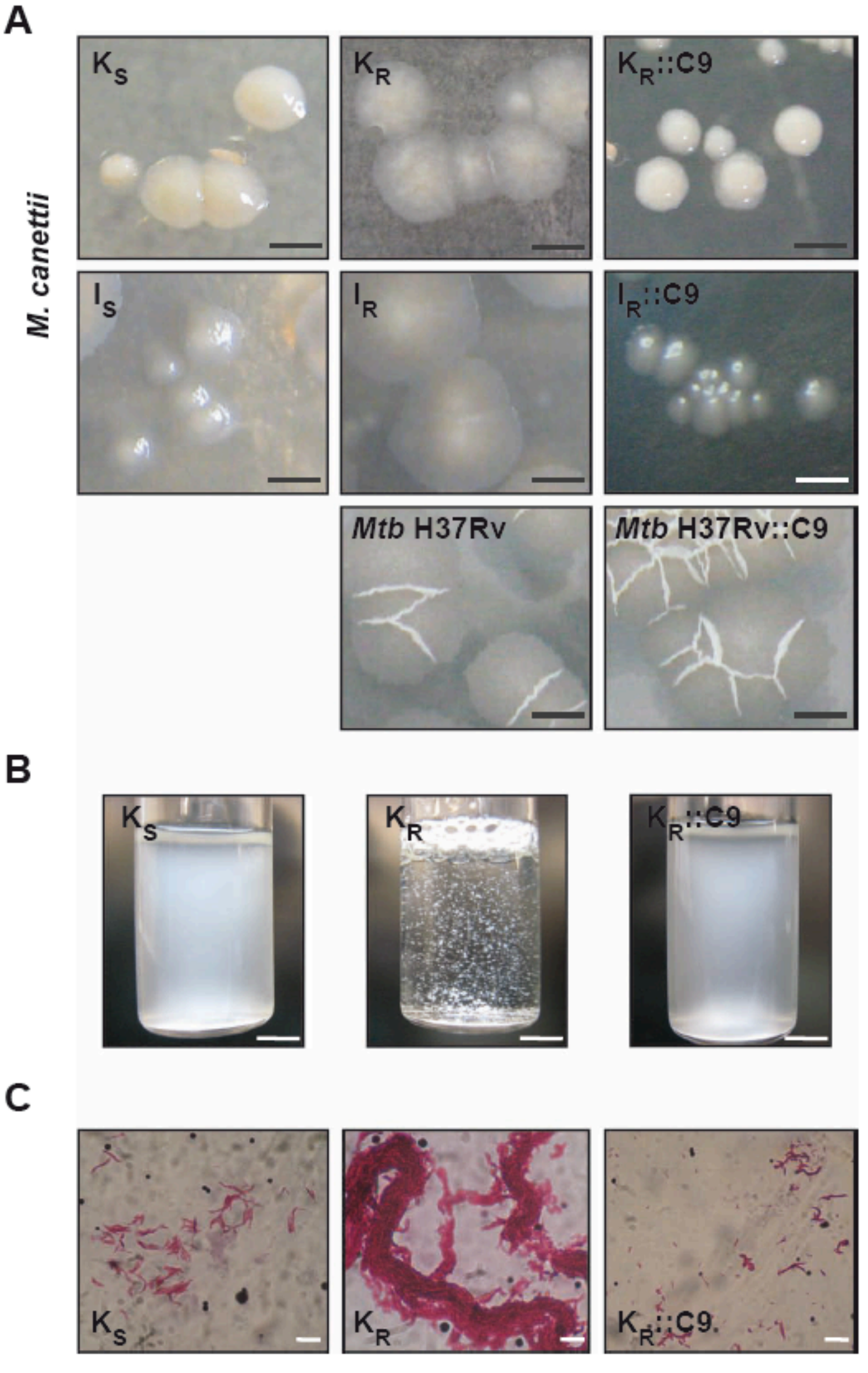
A
M. canettii
K_S
K_R
K_R::C9
I_S
I_R
I_R::C9
Mtb H37Rv
Mtb H37Rv::C9
B
K_S
K_R
K_R::C9
C
K_S
K_R
K_R::C9.

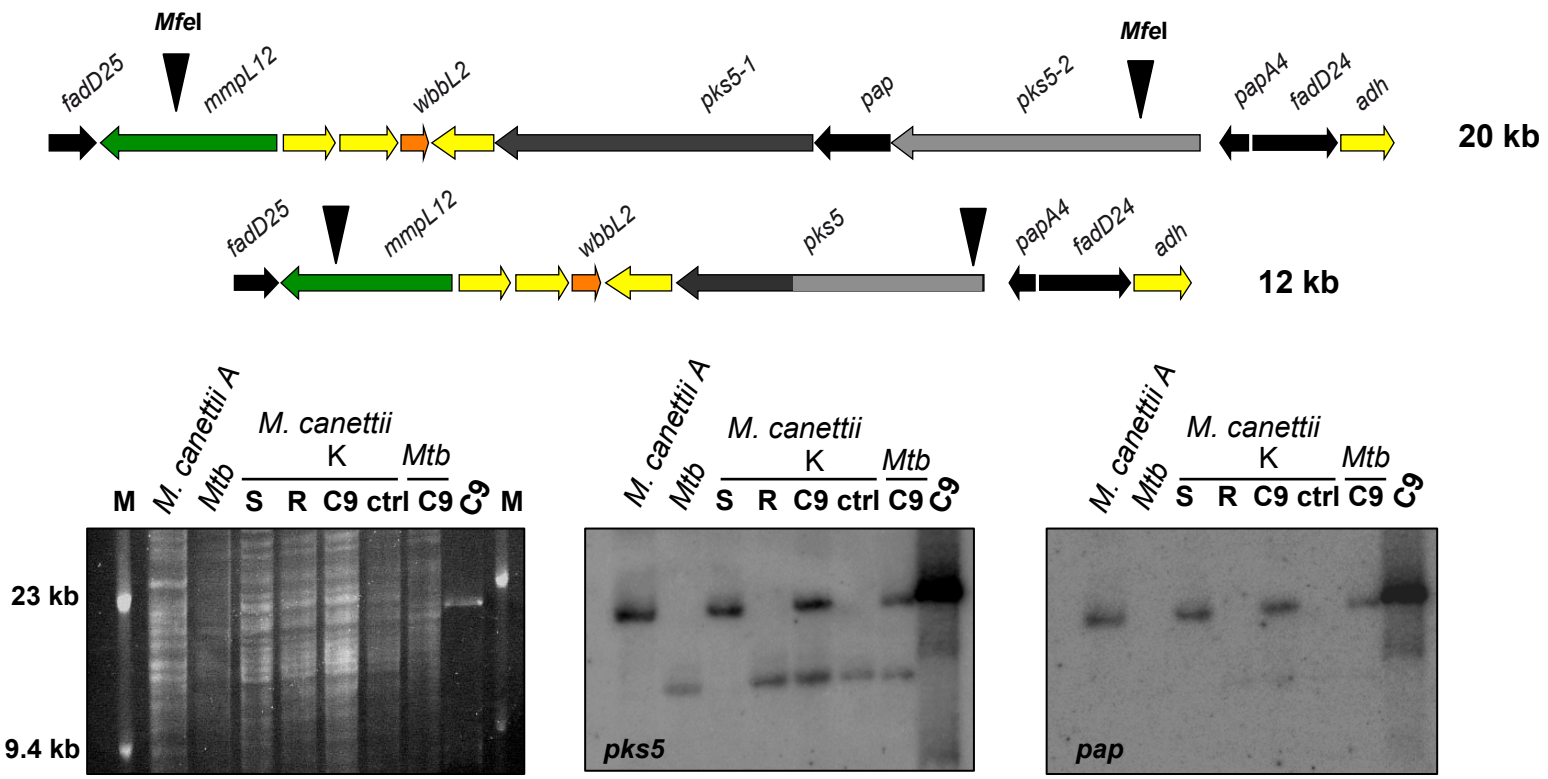
MfeI
fadD25
mmpL12
wbbL2
pks5-1
pap
pks5-2
MfeI
papA4
fadD24
adh
20 kb
fadD25
mmpL12
wbbL2
pks5
papA4
fadD24
adh
12 kb
M. canettii A
M. canettii
K
Mtb
M
S
R
C9 ctrl
C9
C9
M
23 kb
9.4 kb
pks5
pap

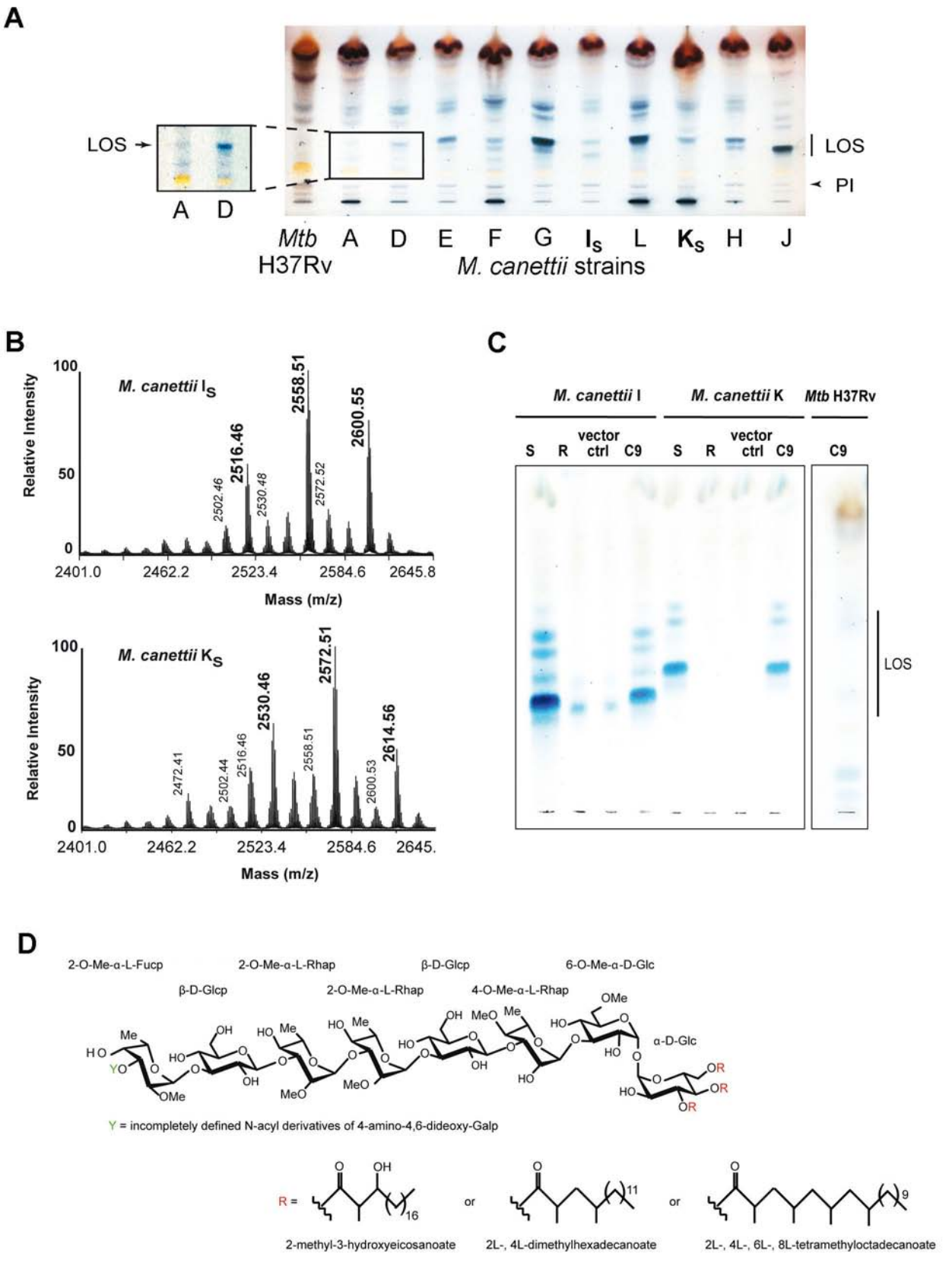
A
LOS
A D
LOS
PI
Mtb H37Rv
A D E F G I_S L K_S H J
M. canettii strains
B
M. canettii I_S
Relative Intensity
100
50
0
2558.51
2600.55
2516.46
2502.46
2530.48
2572.52
2401.0 2462.2 2523.4 2584.6 2645.8
Mass (m/z)
M. canettii K_S
Relative Intensity
2572.51
2530.46
2614.56
2472.41
2502.44
2516.46
2558.51
2600.53
2401.0 2462.2 2523.4 2584.6 2645.
Mass (m/z)
C
M. canettii I
M. canettii K
Mtb H37Rv
S R vector ctrl C9
S R vector ctrl C9
C9
LOS
D
2-O-Me-α-L-Fucp
2-O-Me-α-L-Rhap
β-D-Glcp
6-O-Me-α-D-Glc
β-D-Glcp
2-O-Me-α-L-Rhap
4-O-Me-α-L-Rhap
α-D-Glc
Y = incompletely defined N-acyl derivatives of 4-amino-4,6-dideoxy-Galp
R =
or
or
2-methyl-3-hydroxyeicosanoate
2L-, 4L-dimethylhexadecanoate
2L-, 4L-, 6L-, 8L-tetramethyloctadecanoate

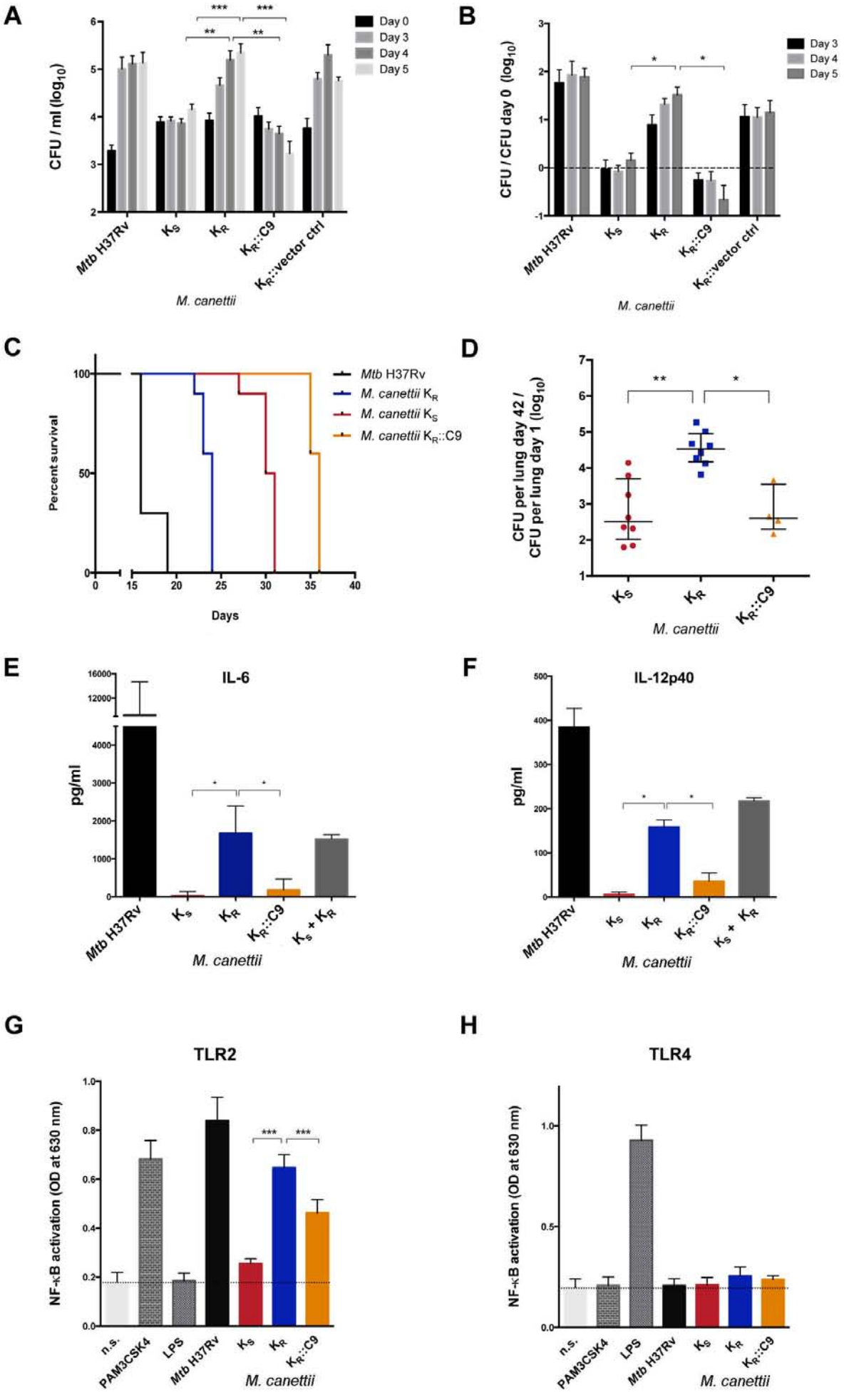
A
CFU / ml (log10)
Day 0
Day 3
Day 4
Day 5
Mtb H37Rv
KS
KR
KR::C9
KR::vector ctrl
M. canettii
B
CFU / CFU day 0 (log10)
Day 3
Day 4
Day 5
Mtb H37Rv
KS
KR
KR::C9
KR::vector ctrl
M. canettii
C
Percent survival
Mtb H37Rv
M. canettii KR
M. canettii KS
M. canettii KR::C9
Days
D
CFU per lung day 42 / CFU per lung day 1 (log10)
KS
KR
KR::C9
M. canettii
E
IL-6
pg/ml
Mtb H37Rv
KS
KR
KR::C9
KS + KR
M. canettii
F
IL-12p40
pg/ml
Mtb H37Rv
KS
KR
KR::C9
KS + KR
M. canettii
G
TLR2
NF-κB activation (OD at 630 nm)
n.s.
PAM3CSK4
LPS
Mtb H37Rv
KS
KR
KR::C9
M. canettii
H
TLR4
NF-κB activation (OD at 630 nm)
n.s.
PAM3CSK4
LPS
Mtb H37Rv
KS
KR
KR::C9
M. canettii

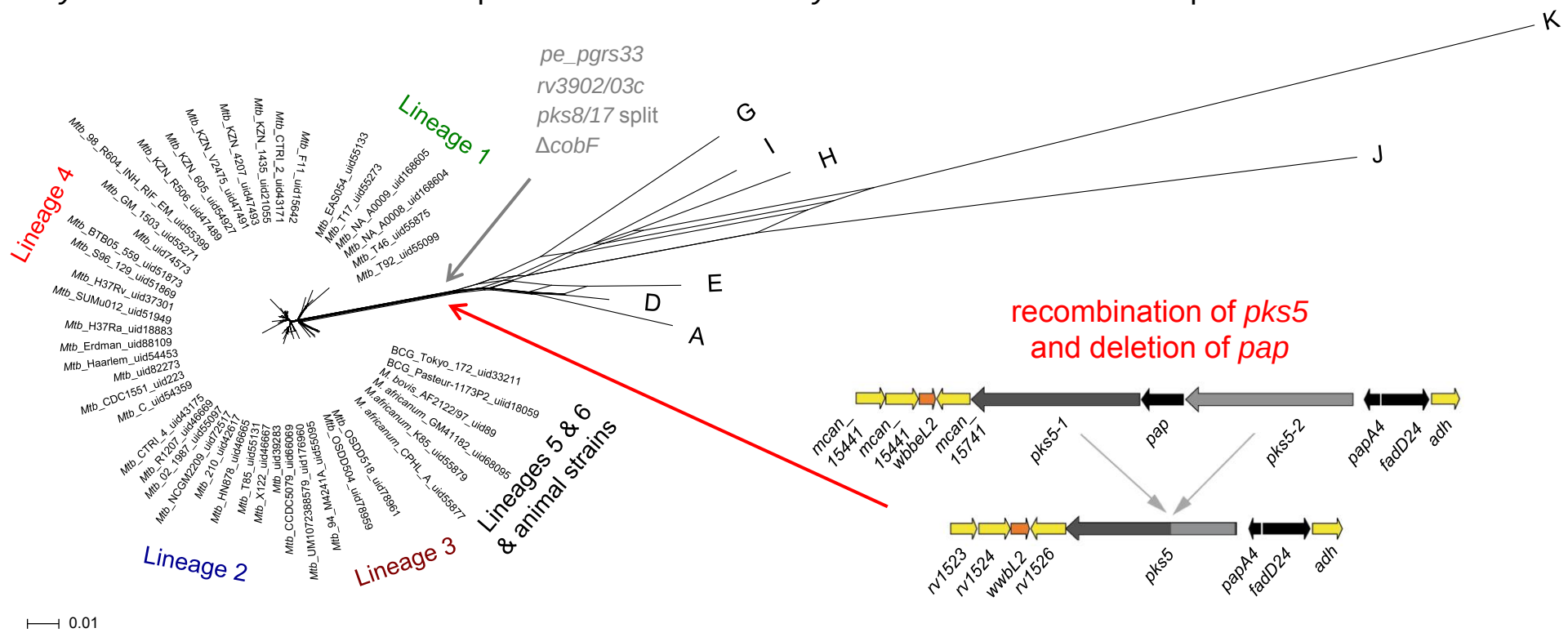
Mycobacterium tuberculosis complex
Mycobacterium canettii strain pool
pe_pgrs33
rv3902/03c
pks8/17 split
Δ*cobF*
Lineage 1
Lineage 2
Lineage 3
Lineage 4
Lineages 5 & 6
& animal strains
K
G
I
H
J
E
D
A
recombination of *pks5*
and deletion of *pap*
mcan_15441
mcan_15441
wbbeL2
mcan_15741
pks5-1
pap
pks5-2
papA4
fadD24
adh
rv1523
rv1524
wwbL2
rv1526
pks5
papA4
fadD24
adh
0.01